

Hard spheres on the gyroid surface

Tomonari Dotera, Masakiyo Kimoto and Junichi Matsuzawa

Interface Focus 2012 2, doi: 10.1098/rsfs.2011.0092 first published online 18 January 2012

This article cites 20 articles, 1 of which can be accessed free References

http://rsfs.royalsocietypublishing.org/content/2/5/575.full.html#ref-list-1

http://rsfs.royalsocietypublishing.org/content/2/5/575.full.html#related-urls

Subject collections Articles on similar topics can be found in the following collections

chemical physics (11 articles)

Receive free email alerts when new articles cite this article - sign up in the box at the top **Email alerting service**

right-hand corner of the article or click here





Interface Focus (2012) **2**, 575–581 doi:10.1098/rsfs.2011.0092 Published online 18 January 2012

Hard spheres on the gyroid surface

Tomonari Dotera^{1,*}, Masakiyo Kimoto¹ and Junichi Matsuzawa²

¹Department of Physics, Kinki University, Higashi-Osaka 577-8502, Japan ²Department of Mathematics, Nara Women's University, Nara 630-8506, Japan

We find that 48/64 hard spheres per unit cell on the gyroid minimal surface are entropically self-organized. Striking evidence is obtained in terms of the acceptance ratio of Monte Carlo moves and order parameters. The regular tessellations of the spheres can be viewed as hyperbolic tilings on the Poincaré disc with a negative Gaussian curvature, one of which is, equivalently, the arrangement of angels and devils in Escher's *Circle Limit IV*.

Keywords: gyroid surface; hard spheres; hyperbolic tiling; ABC star polymer; bicontinuous phase; fluid-solid transition

1. INTRODUCTION

What is the regular arrangement of spheres when a surface is curved? On a flat plane, the hexagonal (equilateral-triangular) arrangement is ubiquitous from microscopic objects (e.g. electrons, atoms and molecules) to mesoscopic objects (e.g. liquid crystals, polymers and colloidal particles). The arrangement stems from the densest packing of hard spheres, space division or interactions between particles; for instance, the Coulombic force between electrons organizes the Wigner crystal. For surfaces with positive Gaussian curvatures, remarkable arrangements are observed in fullerenes and icosahedral capsids. Furthermore, the distribution problem of electrons on a sphere has been considered for many years as the 'Thomson problem' [1]. In contrast, a regular arrangement on a saddle-shaped (hyperbolic) surface with negative curvatures has not been identified in soft materials; one regular arrangement so far discovered is in inorganic mesoporous materials [2].

Nearly 30 years ago, Rubinstein & Nelson [3] addressed the problem of hard discs on surfaces with constant negative curvatures as an analogue of frustrated sphere packing in three-dimensional space. Furthermore, Modes & Kamien [4] calculated virial coefficients of hard discs on surfaces with constant negative curvatures to determine the equation of states. Unfortunately, however, a plane with a constant negative curvature mathematically cannot be realized in Euclidian three-dimensional space. Instead of constant negative curvatures, triply periodic saddle-shaped surfaces with non-positive curvatures such as gyroid [5], diamond and primitive surfaces are found in various soft materials such as biological lipids, surfactants, mesoporous materials, and block copolymers [6–9]. Recently, it was found that polyisoprene spheroids spread over a polystyrene gyroidal membrane in an ABC star block copolymer melt [10]. Moreover, regulated membranes can act as scaffolds to construct more complex structures [11,12]. Therefore, it is worth studying regular

One contribution of 18 to a Theme Issue 'Geometry of interfaces: topological complexity in biology and materials'.

arrangements on such triply periodic saddle-shaped surfaces [13].

On a flat plane, a fluid—solid transition occurs even for the purely hard-sphere potential because of the excess entropy of the regular arrangement [14]. Namely, above a certain critical density, the crystalline arrangement of spheres gains more entropy than the random arrangement gains. Is there a similar transition on the gyroid surface? Here, we report the results of Monte Carlo simulations of entropy-driven order—disorder transitions on the surface, and propose a regular arrangement on the gyroid surface.

2. MONTE CARLO SIMULATION

2.1. Method

We consider hard spheres whose centres are confined in a rigid gyroidal membrane. The well-known approximation form of the gyroid surface is shown by

$$g(\mathbf{r}) = \sin x \cos y + \sin y \cos z + \sin z \cos x, \quad (2.1)$$

where we omit a factor $2\pi/a$ for x, y and z [15]. Hereafter, we choose the lattice constant a=1. For simulations, we employ a gyroid membrane $|g(\mathbf{r})| \leq 0.1$, whose boundaries are given by g(r) = -0.1 (green) and g(r) = 0.1 (red) as shown in figure 1.

Monte Carlo simulations are conducted with sizes (ha, ka, la), where $1 \le h, k, l \le 3$. We assign N(N=48-64) to the number of hard spheres per unit cell, and the total number of spheres M in a simulation box with (h, k, l) is M=hklN. Periodic boundary conditions for x, y and z directions are exerted. We prepare M spheres whose centres are within $|g(\mathbf{r})| \le 0.1$ without hard contact. This condition is easily achieved when the radius is small.

The Monte Carlo procedure is as follows. (i) Select a sphere randomly. (ii) Generate a trial move within a box whose sizes Δx , Δy and $\Delta z = \pm 0.0075$ by the uniform distributions. (iii) Reject the trial move if $|g(\mathbf{r})| > 0.1$ or there is any hard contact with other spheres; if not, accept the move. (iv) Return to (i). (v) Record the acceptance ratio and the value of an order parameter. At each radius, 10^6 Monte Carlo

^{*}Author for correspondence (dotera@phys.kindai.ac.jp).

Figure 1. Gyroidal surfaces with g(r) = -0.1 (green) and g(r) = 0.1 (red). The centres of spheres are confined between the surfaces for simulations.

0.5

0

steps are carried out. (vi) Change the radius of spheres upward; the increment is 0.0001. For N=48 and N=64, decreasing paths from regular arrangements are also performed.

Let us make a few remarks. (i) The principle of detailed balance of Monte Carlo moves is guaranteed by the above procedures. (ii) The distance between two spheres is measured in terms of the three-dimensional Euclidean distance, not the geodesic distance on the hyperbolic surface, i.e. we simulate hard spheres not discs. (iii) The thickness of the membrane is not exactly uniform, but it is thinner than the radii under consideration. Thus, we presume that this does not affect the key feature of the results.

In order to see order—disorder transitions for N = 48 and N = 64, we measure order parameters h(r) as a function of radius r defined by

$$h(r) = \left\langle \frac{1}{M} \sum_{i=1}^{M} f(\mathbf{r}_i) \right\rangle,$$

where the sum is taken over all spheres in question, and $\langle \cdots \rangle$ implies the Monte Carlo average. The function $f(\mathbf{r})$ for N=48 is $f_{48}(\mathbf{r})$, which is a function of the position of sphere centres, shown by

$$f_{48}(\mathbf{r}) = \sin 2x \sin 2y \sin 4z + \sin 2x \sin 4y \sin 2z + \sin 4x \sin 2y \sin 2z.$$

The absolute value of this function takes a large value when the positions of the spheres are in regular arrangement. Technically, the function $f_{48}(\mathbf{r})$ is generated by the Fourier transform of all generic points of the space group $I\bar{4}3d$ for the (h, k, l) = (4, 2, 2) peak, and thus are invariant under the operations of $I\bar{4}3d$ [16]. In figure 2, level set surfaces defined by $f_{48}(\mathbf{r}) = \pm 0.8$ are displayed, together with the regular arrangement. There are two choices of regular arrangement for N = 48, which can be expressed by the sign of the function. As shown in figure 2, the regular positions

match well with those of the level surfaces. We note that equation (2.1) is obtained from $I4_132$ and (h, k, l) = (2, 1, 1) in the same way as mentioned above [15]. Since the regular positions for N=64 are divided into two symmetrically inequivalent groups, a simple function as good as $f_{48}(\mathbf{r})$ could not be constructed. Thus, we temporary calculate the order parameter by using

$$f_{64}(\mathbf{r}) = (\cos 4x + \cos 4y + \cos 4z + \cos x \sin y \sin 2z + \cos y \sin z \sin 2x + \cos z \sin x \sin 2y)^2,$$

where the first three terms express Wyckoff position 16a sites and the last three terms express 48g sites for $Ia\bar{3}d$. It turns out that the function is useful near the transition region.

2.2. Results

1.0

The existence of a transition is judged by whether or not there is a jump in the acceptance-ratio curve. We have obtained sound evidence for N = 64. Figure 3a displays the acceptance ratio of Monte Carlo moves for the system with (h, k, l) = (2, 2, 3); namely, 768 (64/per unit cell) hard spheres whose centres are on the gyroid surface. Upon increasing the radius of spheres, the curve basically decreases because of the increase in contacts. However, at about r = 0.105, the ratio abruptly jumps up about 0.08. This is the transition from the disordered state to the ordered state. We render the order parameter h(r) in figure 3b, which shows a jump at the same radius. When starting from a regular structure described in §3, both upward and downward curves trace the same curve above $r \sim$ 0.106, then the downward curve exceeds the transition point at r = 0.105 like superheating. The curve shows an abrupt downturn at approximately r = 0.101. This hysteresis is typical evidence of the first-order transition. We illustrate a snapshot of the result just above the transition in figure 4a. Note that we have observed jumps for the simulation boxes with (h, k, k)(1, 1, 1), (1, 1, 2), (1, 2, 2), (2, 2, 2), (1, 1, 3)(2, 3), (2, 2, 3),and (1, 3, 3).In the series, the upward transition radius turns out to increase a little with the size of boxes tending to converge, while the downward transition radius is almost constant. The box size seems to be limited by simulation time.

In the case of N = 48, however, we have seen transitions for (h, k, l) = (1, 1, 1) and (1, 1, 3). Using our computational power, we find that the transition is not easily accessible to us. As we have mentioned, there are two possible regular configurations for N=48, which may cause the difficulty. Therefore, we have added a solid region (green shaded box) as shown in figure 4b for (hkl) = (2, 3, 3) to enhance the transition. The spheres in the region $(0 \le z \le 1)$ are fixed on regular sites that acted as a solid interface. As shown in figure 3c, it exhibits an entropy-driven fluid-solid transition when the radius of spheres was greater than approximately 0.118 in the unit of the lattice constant. In figure 3d, the order parameter measured in the region $(1.5 \le z < 2.5)$ is a monotonically increasing function of sphere radius and the maximum value is 1.473. Figure 4b displays self-organized 864 (48/per unit

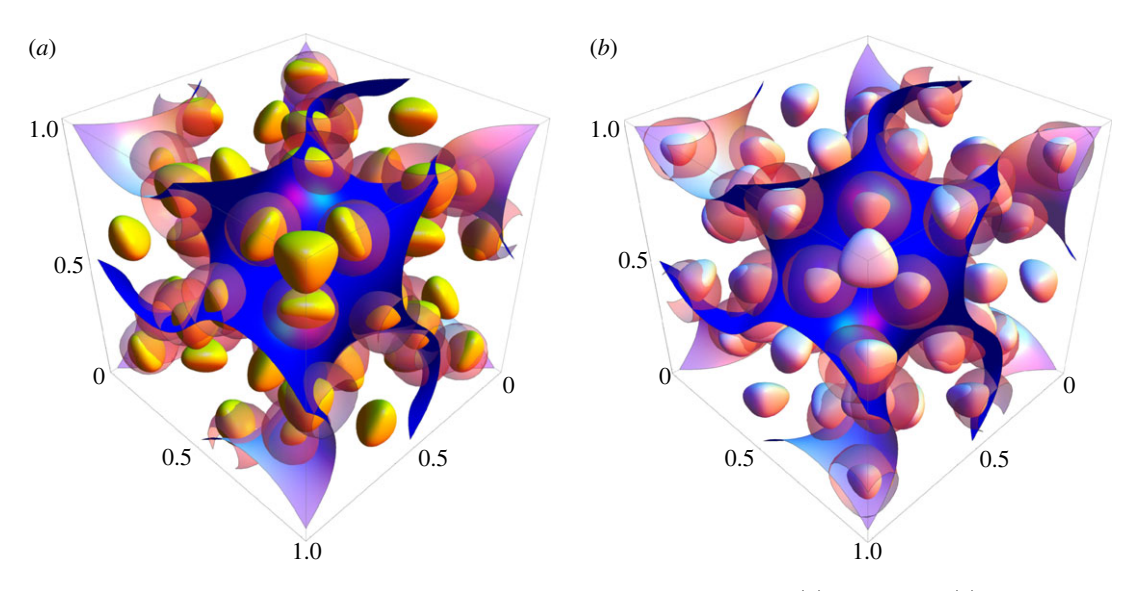


Figure 2. Transparent spheres indicate two types of regular arrangement for N = 48: (a) minus and (b) plus. The level surfaces $f_{48}(\mathbf{r}) = -0.8$ (in yellow) and $f_{48}(\mathbf{r}) = 0.8$ (in pink) are superimposed.

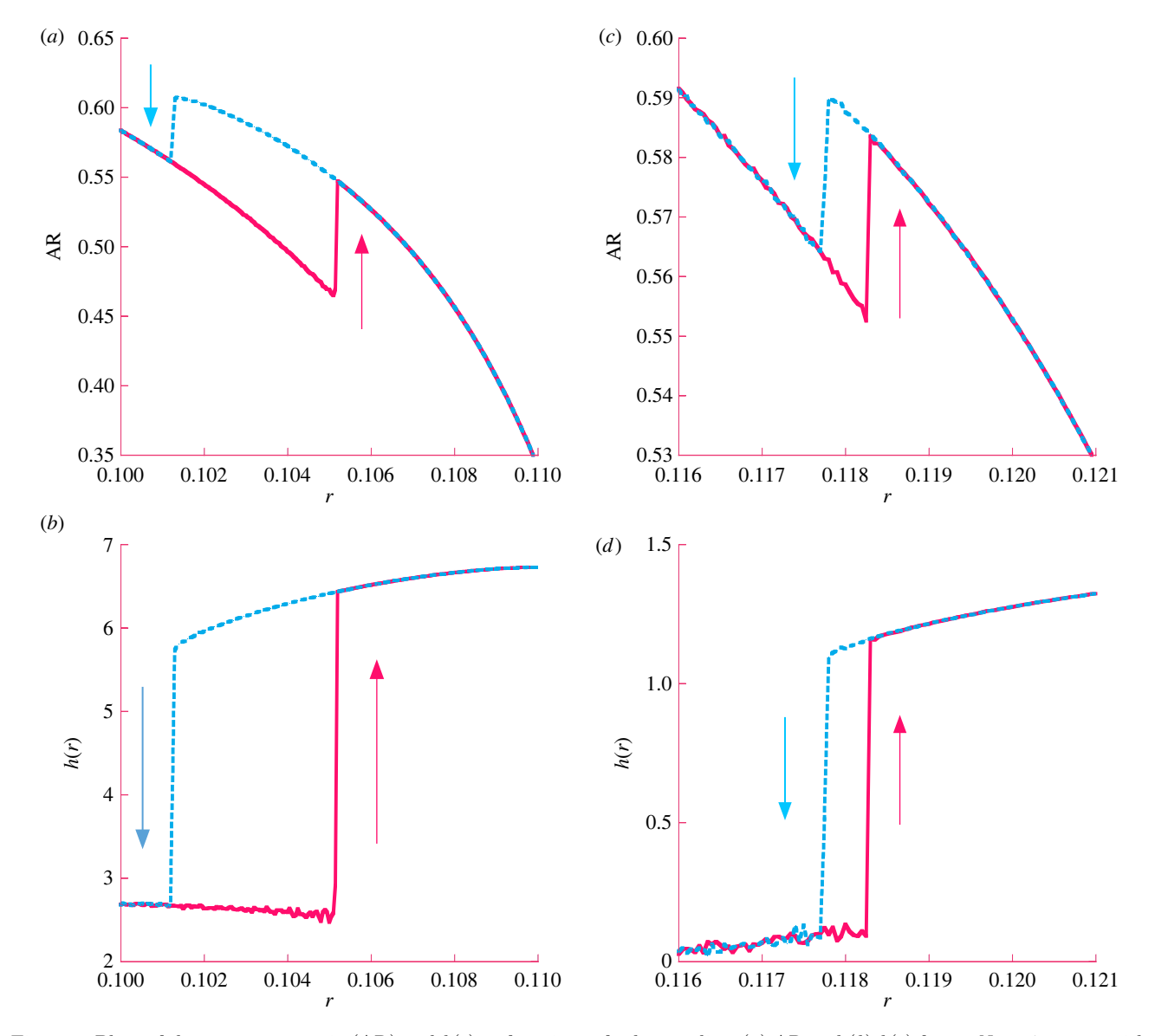


Figure 3. Plots of the acceptance ratio (AR) and h(r) as functions of sphere radius. (a) AR and (b) h(r) for an N = 64 system with (h, k, l) = (3, 2, 2). (c) AR and (d) h(r) for an N = 48 system with (3, 3, 2). (a-d) Solid line, up; dashed line, down.

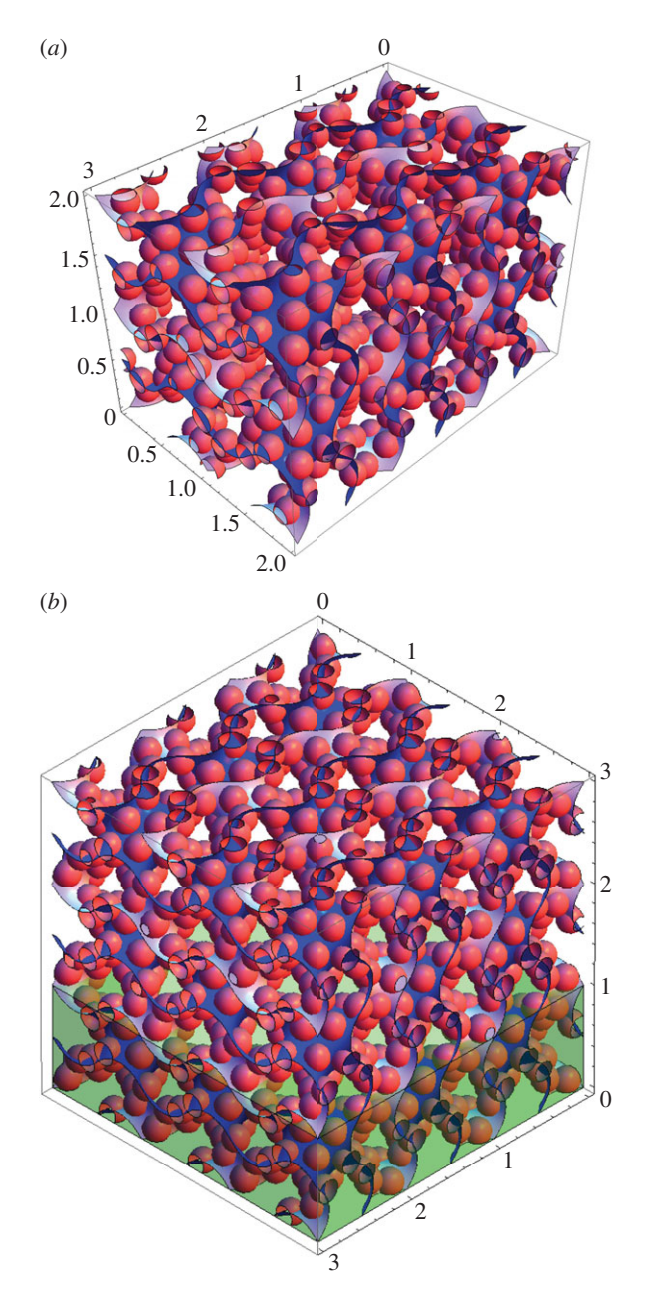


Figure 4. Self-organized spheres on the gyroid surface for (a) an N=64 system with (h, k, l)=(3, 2, 2), and (b) an N=48 system with (h, k, l)=(3, 3, 2). These configurations correspond to (a) $(3^6; 3^2.4.3^2.4)$ and (b) $(3^3.4.3.4)$. In (b) one-third of the spheres at the bottom (shaded by green) are fixed as a solid region.

cell) hard spheres. Without the solid region, we have found random configurations frustrated with two (+ and -) tilings, which end up with glassy states.

It turns out that jumps seem to exist for N=48, 52, 59, 60, 61, 62, 63 and 64 in the case of the smallest box (1, 1, 1), although curves fluctuate considerably at the transition regions. We have conducted a systematic investigation and found that, except for (1, 1, 1), there is no order–disorder transitions in the range of 48 < N < 64.

3. HYPERBOLIC TILING

To analyse tessellations on the gyroid surface, we use hyperbolic tiling [17-21]. A hyperbolic tiling is the

hyperbolic analogue of a tiling on a plane, and is usually depicted on the Poincaré disc representing hyperbolic geometry: a household example is Escher's enchanting series of artworks Circle Limit. More than two decades ago, Charvolin and Sadoc pointed out that the Poincaré disc in figure 5 tiled by $(\pi/2, \pi/4, \pi/6)$ -triangles is group-theoretically related to the gyroid surface. The dodecagonal region within 12 thick curves in figure 5 can be conformally mapped upon the gyroid surface and cover half the area of the surface in a unit cell. A useful fact is that the symmetry operation of $Ia\bar{3}d$ is lifted to the orientation-preserving group action in figure 5.

We propose three regular arrangements: (1) a monohedral triangular tiling $(3^6; 3^8)$; (2) an Archimedean tiling $(3^3.4.3.4)$ [22]; and (3) a tiling $(3^6; 3^2.4.3^2.4)$ consisting of 40, 48 and 64 vertices per unit cell on the gyroid surface. The set of integers $(n_1 \cdot n_2 \cdot n_3 \cdot \ldots)$ denotes tiling of a vertex type in the way that n_1 -gon, n_2 -gon and n_3 -gon, ... meet consecutively on each vertex, and superscripts are employed to abbreviate when possible. A set of integers such as $(3^6; 3^8)$ denotes a tiling composed of two vertex types 3^6 and 3^8 , for instance. We presume that these tilings are hyperbolic extensions of the flat plane tessellation (3^6) .

- (1) Vertex positions of hyperbolic monohedral $(3^6; 3^8)$ tiling are located at the site symmetry points, $.\bar{3}$. and $\bar{4}$.. of space group $Ia\bar{3}d$ (no. 230). The corresponding points are denoted as 16a and 24d sites, representing multiplicity and the Wyckoff letter. The red and yellow circles in figure 5 correspond to Wyckoff positions of $Ia\bar{3}d$, 16a and 24d, respectively, whose positions are geometrically monkey and horse saddle points of the gyroid surface. The space group of $(3^6; 3^8)$ is $Ia\bar{3}d$ (no. 230).
- (2) Each centre of shaded triangles made by one 16a and two 24d positions corresponds to a vertex of a $(3^3 .4.3.4)$ tiling (figure 5a). Since the mapping preserves local connectivity, every vertex of $(3^3.4.3.4)$ tiling has six neighbours and the same local environment. Thus, we call it Archimedean tiling even for hyperbolic geometry. The whole area is divided into alternating white and grey regions in figure 5a, and correspondingly the inversion symmetry of Ia3d is broken. This procedure enables us to find a curious coincidence between the tessellation of green circles in figure 5a and that of angels (or devils) in Escher's Circle Limit IV. In the three-dimensional space, the positions are (0.576, 0.386, 0.554) and its symmetry equivalents. Remarkably, the distance between the nearest spheres is the same. Fortyeight vertex positions of the tiling in figure 6a,b are generated by symmetry operations of space group $I\overline{4}3d$ (no. 220), which is one of the cubic subgroups of $Ia\bar{3}d$, but different from $I4_1\bar{3}2$ (no. 214) associated with the single-gyroid phase.
- (3) The space group of $(3^6; 3^2.4.3^2.4)$ is $Ia\bar{3}d$. The tiling composed of 64 vertices per unit cell is shown in figure 6c,d. Notice that the tiling consists of two types of vertices: one of which is 16a, a site symmetry point $.\bar{3}$. of space group $Ia\bar{3}d$; the other

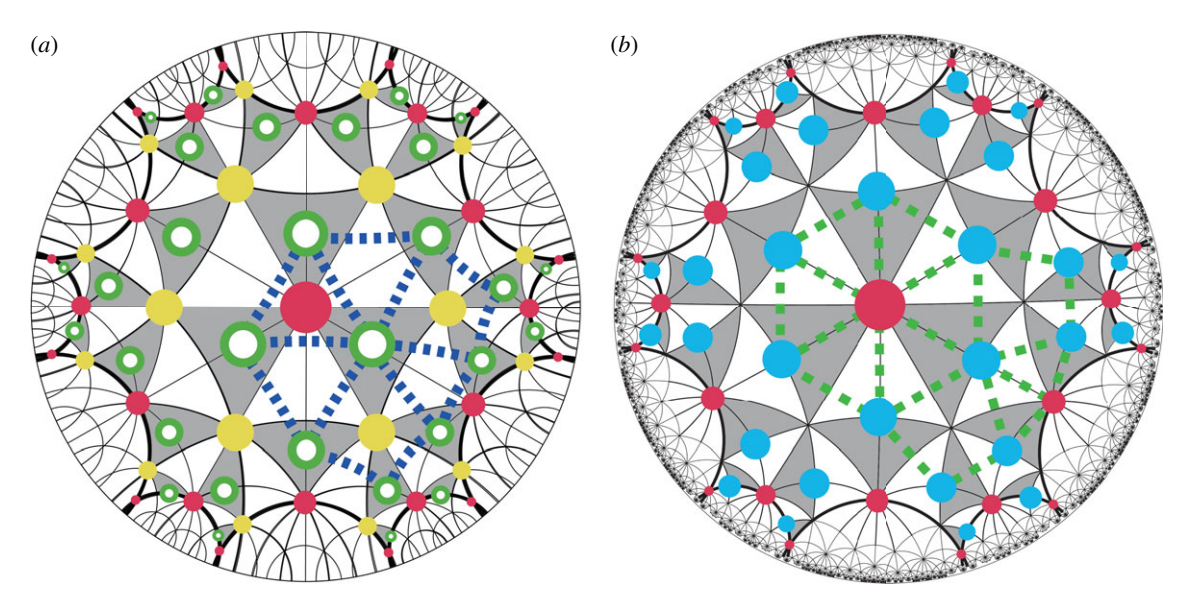


Figure 5. Poincaré disc tiled with $(\pi/2, \pi/4, \pi/6)$ -triangles (halves of white or shaded ones). The dodecagonal region within 12 thick curves can be conformally mapped on the gyroid surface and cover half the area of the surface in a unit cell. Then red, yellow and blue circles correspond to Wyckoff positions of $Ia\bar{3}d$, 16a, 24d and 48g, respectively. (a) Green open circles in shaded triangles correspond to vertices of the $(3^3.4.3.4)$ tiling (blue dotted lines), corresponding to the N=48 system. (b) Red (3^6) and blue $(3^2.4.3^2.4)$ circles correspond to vertices of the $(3^6; 3^2.4.3^2.4)$ tiling (green dotted lines), corresponding to the N=64 system.

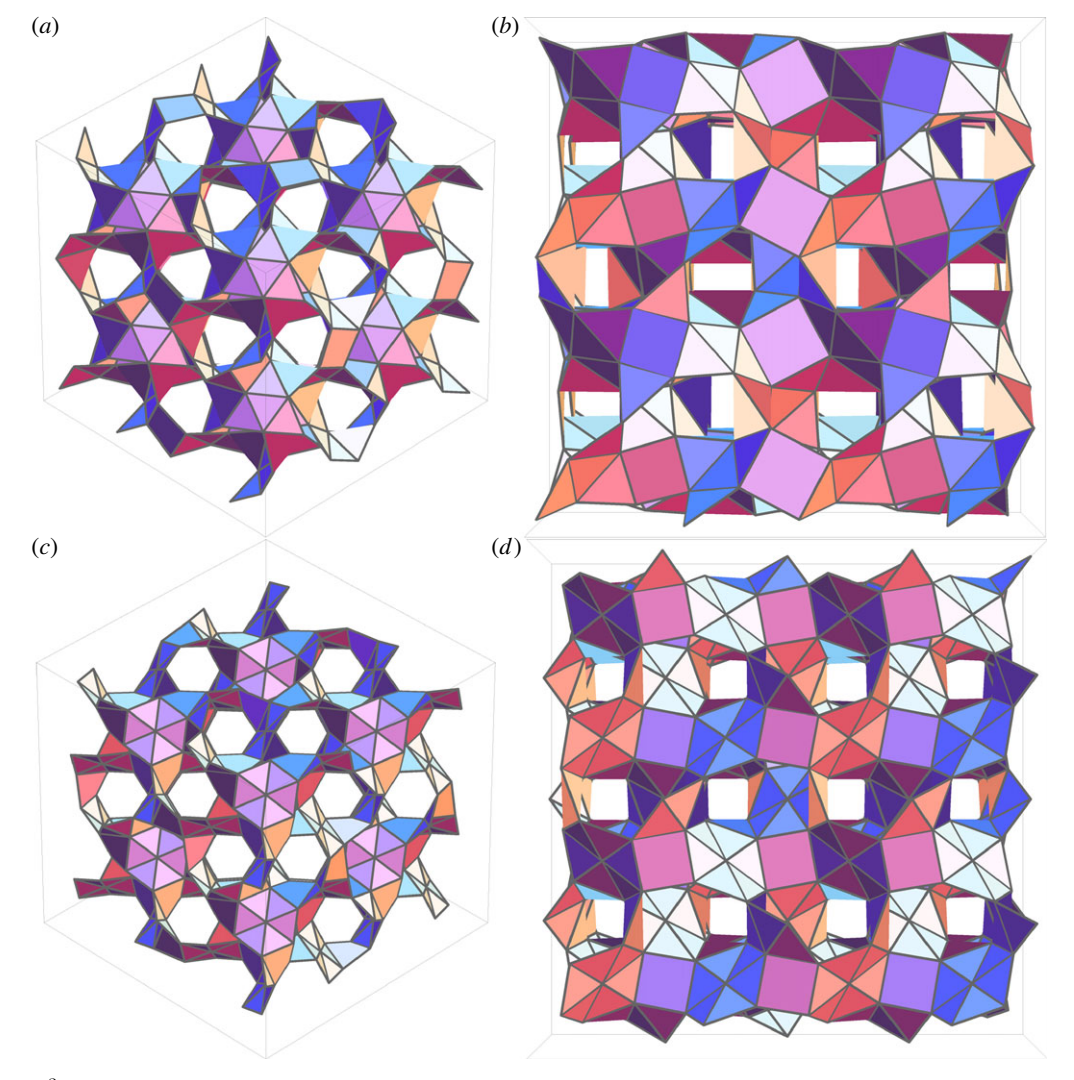


Figure 6. (a,b) (3³.4.3.4) Archimedean tiling with 48 vertices per unit cell, in a two-periodic cell viewed from (a) [111] and (b) [100] directions. (c,d) (3⁶; 3².4.3².4) tiling with 64 vertices per unit cell, in a two-periodic cell viewed from (c) [111] and (d) [100] directions.

type is 48g, a site symmetry point ...2; here, the position is precisely given by $(\frac{1}{8}, y, \bar{y} + \frac{1}{4})$ with y =0.337 [23] and its symmetry equivalents. Notice that the 16a points are surrounded by six isosceles triangles (not equilateral triangles); thus, the hexagon consisting of the six triangles is not flat as shown in the central part of figure 6c.

4. DISCUSSION

Remarkably, the entropy-driven transition of hard spheres on the gyroid surface occurs. Because the acceptance ratio only reflects local entropy, it is not the total configurational entropy. However, since there is no energetic term, the jump in the ratio implies entropic ordering. This kind of entropic-ordering principle prevails among many soft-matter systems.

Why do N = 48 and N = 64 systems order? For N=48, the property of equidistance (0.259 in the unit of the lattice constant) seems to be advantageous to entropic ordering, because the same free volume for all spheres gives the maximum entropy when it is assumed that each sphere is confined in the Voronoi cell, although the relation between the free-volume cell and the Voronoi cell is not straightforward in the presence of a curved background [13]. Furthermore, there exist a point and its symmetry equivalents on the gyroid surface calculated even by the Weierstrass-Enneper representation such that all edge lengths take the same value [22]. The same property holds for N = 64, since the edge-length difference is within 1.1 per cent (the equidistant points are given by y = 5/16 for 48g sites, but not on the gyroid surface). Because of this geometric condition, the symmetry governs the self-organization for N=48 and N=64. In future, it will be interesting to see the relation between the packing fractions of spheres (or discs) at transitions and those of the densest packing for a given N.

We have elucidated that the regular tessellations of the spheres can be viewed as hyperbolic tilings on the Poincaré disc or regular tiling structures in the Euclidean space. We emphasize that, as investigated by several researchers, the Poincaré disc and three-dimensional nets are useful to understand the symmetry and the regulated structures on the gyroid surface. We point out that adding squares in triangle tilings is a plausible way to form regular structures relating to the gyroid structure. Squares are not so unrealistic because square—triangle tilings have been observed in ABC star block terpolymers [24,25]; as mentioned above, the monohedral tiling (3⁶;3⁸) is possible, though. In addition, another Archimedean (3⁷) net is possible; however, when the distance is the same, it contains tetrahedrons and it is not on the gyroid surface.

We hope that this study may hint at why the hyperbolic tiling structure can form in an ABC star block copolymer melt, and we consider that the new tiling structures obtained are plausible structural candidates.

This work was supported by the Grant-in-Aid for Scientific Research (C) (no. 22540375) from JSPS, Japan, and the Grant-in-Aid for Scientific Research on Priority Areas

(no. 20045006) from MEXT, Japan. T.D. is grateful to Y. Matsushita, A. Takano, K. Hayashida and N. Fujita.

REFERENCES

- 1 Thomson, J. J. 1904 On the structure of the atom: an investigation of the stability and periods of oscillation of a number of corpuscles arranged at equal intervals around the circumference of a circle; with application of the results to the theory of atomic structure. Phil. Mag. **7**, 237–265.
- 2 Zou, X., Conradsson, T., Klingstedt, M., Dadachov, M. S. & O'Keeffe, M. 2005 A mesoporous germanium oxide with crystalline pore walls and its chiral derivative. *Nature* **437**, 716-719. (doi:10.1038/nature04097)
- 3 Rubinstein, M. & Nelson, D. R. 1983 Dense-packed arrays on surfaces of constant negative curvature. Phys. Rev. B 28, 6377-6386. (doi:10.1103/PhysRevB.28.6377)
- 4 Modes, C. D. & Kamien, R. D. 2007 Hard disks on the hyperbolic plane. Phys. Rev. Lett. 99, 235701. (doi:10. 1103/PhysRevLett.99.235701)
- 5 Schoen, A. H. 1970 Infinite periodic minimal surfaces without self-intersections. Technical Note NASA-TN-D-5541, NASA, Washington, DC.
- 6 Gòzdz, W. & Hołyst, R. 1996 From the plateau problem to periodic minimal surfaces of lipids, surfactants and diblock copolymers. *Macromol. Theory* 321-332. (doi:10.1002/mats.1996.040050212)
- 7 Hyde, S., Andersson, S., Larsson, K., Blum, Z., Landh, T., Lidin, S. & Ninham, B. 1997 The language of shape. Amsterdam, The Netherlands: Elsevier.
- 8 Deng, Y. & Mieczkowski, M. 1998 Three-dimensional periodic cubic membrane structure in mitochondria of amoebae Chaos carolinensis. Protoplasma 203, 16-25. (doi:10.1007/BF01280583)
- 9 Terasaki, O. (ed.) 2004 Mesoporous crystals and related nano-structured materials. Amsterdam, The Netherlands: Elsevier.
- 10 Matsushita, Y., Hayashida, K., Dotera, T. & Takano, A. 2011 Kaleidoscopic morphologies from ABC star-shaped terpolymers. J. Phys. Condens. Matter 23, 284111. (doi:10.1088/0953-8984/23/28/284111)
- 11 Dinsmore, A. D., Hsu, M. F., Nikolaides, M. G., Marquez, M., Bausch, A. R. & Weitz, D. A. 2002 Colloidosomes: selectively permeable capsules composed of colloidal particles. Science 298, 1006–1009. (doi:10.1126/science.1074868)
- 12 Baumgart, T., Hess, S. T. & Webb, W. W. 2003 Imaging coexisting fluid domains in biomembrane models coupling curvature and line tension. Nature 425, 821–824. (doi:10. 1038/nature02013)
- 13 Modes, C. D. & Kamien, R. D. 2008 Geometrical frustration in two dimensions: idealizations and realizations of a hard-disk fluid in negative curvature. Phys. Rev. E 77, 041125. (doi:10.1103/PhysRevE.77.041125)
- 14 Alder, B. J. & Wainwright, T. E. 1957 Phase transition for a hard sphere system. J. Chem. Phys. 27, 1208–1209.
- 15 von Schnering, H. G. & Nesper, R. 1991 Nodal surfaces of Fourier series: fundamental invariants of structured matter. Z. Phys. B Condens. Matter 83, 407-412. (doi:10.1007/BF01313411)
- 16 Wohlgemuth, M., Yufa, N., Hoffmann, J. & Thomas, E. L. 2001 Triply periodic bicontinuous cubic microdomain morphologies by symmetries. Macromolecules 34, 6083-6089. (doi:10.1021/ma0019499)
- 17 Hilbert, D. & Cohn-Vossen, S. $1932\ Geometry\ and\ the$ imagination. Providence, RI: American Mathematical Society. (Reprint edition 1999.)

- 18 Charvolin, J. & Sadoc, J. F. 1987 Periodic systems of frustrated fluid films and bicontinuous cubic structures in liquid crystals. J. Physique 48, 1559-1569. (doi:10.1051/ jphys:019870048090155900)
- Mackay, A. L. & Terrones, H. 1991 Diamond from graphite. Nature 352, 762. (doi:10.1038/352762a0)
- 20 Nesper, R. & Leoni, S. 2001 On tilings and patterns on hyperbolic surfaces and their relation to structural chemistry. Chem. Phys. Chem. 2, 413-422. (doi:10. 1002/1439-7641(20010716)2:7 < 413::AID-CPHC413 > 3.3.CO;2-M)
- 21 Ramsden, S. J., Robins, V. & Hyde, S. T. 2009 Three-dimensional Euclidean nets from two-dimensional hyperbolic tilings: kaleidoscopic examples. Acta Cryst. A **65**, 81–108. (doi:10.1107/S0108767308040592)

- 22 Dotera, T. & Matsuzawa, J. 2011 Hyperbolic tiling on the gyroid surface in a polymeric alloy. Kokyuroku, RIMS, Kyoto Univ. 1725, 80-91.
- 23 Hahn, T. ed. 2002 International tables for crystallography. Vol. A. Space group symmetry, 5th edn, 2nd printing. New York, NY: Springer.
- 24 Takano, A., Kawashima, W., Noro, A., Isono, Y., Tanaka, N., Dotera, T. & Matsushita, Y. 2005 A mesoscopic archimedean tiling having a new complexity in an ABC star polymer. J. Polym. Sci. Part B Polym. Phys. 43, 2427-2432. (doi:10. 1002/polb.20537)
- 25 Hayashida, K., Dotera, T., Takano, A. & Matsushita, Y. 2007 Polymeric quasicrystal: mesoscopic quasicrystalline tiling in ABC star polymers. Phys. Rev. Lett. 98, 195502. (doi:10.1103/PhysRevLett.98.195502)